ACS Macro Letters

Letter

pubs.acs.org/macroletters

Elucidating Water Transport Mechanisms in Nafion Thin Films

Eric M. Davis,* Christopher M. Stafford, and Kirt A. Page*

Materials Science and Engineering Division, National Institute of Standards and Technology, Gaithersburg, Maryland 20899, United States

Supporting Information

ABSTRACT: Ion-exchange membranes are critical components of hydrogen fuel cells, where these ionomers can be confined to nanoscale thicknesses, altering the physical properties of these films from that of bulk membranes. Therefore, it is important to develop methods capable of measuring and elucidating the transport mechanisms under thin film confinement compared to bulk Nafion. In this study, water sorption and diffusion in a Nafion thin film were measured using time-resolved in situ polarization modulation infrared reflection absorption spectroscopy (PM-IRRAS). Interfacial mass transport limitations were confirmed to be minimal, while restricted water diffusion was observed, where the effective diffusion coefficient of water in the thin Nafion film was many orders of magnitude lower (between 4 and 5 orders of magnitude) than those reported for bulk membranes and was dependent on the initial hydration state of the Nafion. Furthermore, the response of the hydrophobic domains (Teflon backbone) to the swelling of the hydrophilic domains (ionic clusters) was shown to be orders of magnitude slower than that of bulk Nafion.

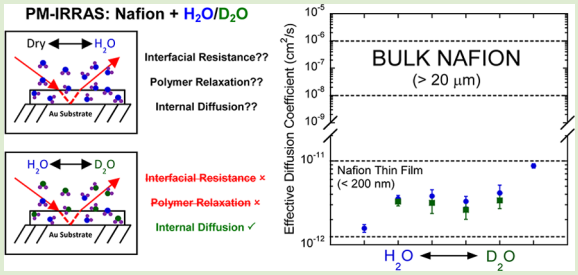

Proton exchange membrane (PEM) fuel cells have emerged as a promising energy conversion technology for automotive transportation, as well as many other applications that require clean, quiet, and portable power.[1,2] In recent years, perfluorosulfonic acid (PFSA) has proven to be the most widely used membrane material for PEM fuel cells.[3] Nafion,[4] a PFSA membrane that is comprised of a Teflon backbone with perfluorvinyl ether side-chains, terminated by sulfonic acid groups, is currently the industrial standard for PEMs as a result of its high proton conductivity and good chemical and thermal stability.[5] The flexibility and polarity of the side chains results in nanophase separation from the hydrophobic backbone, creating a complex morphological structure, which plays a critical role in determining the transport properties of Nafion films. Furthermore, the location of the Nafion within the fuel cell ultimately determines whether this ionomer is found on micron or nanometer size-scales. Current synthesis methods of gas diffusion electrodes for fuel cells include incorporation of the Nafion in the catalyst ink as an ionic conducting binder, thus creating confined, nanoscale Nafion films.[6,7] Proton conductivity in these Nafion membranes is inherently coupled to the level of hydration, where water management within the film is governed by the water transport mechanisms present in Nafion. With this, polymer structure/dynamics and water/proton transport in thin Nafion films have become important areas of research.[5,8−20]

Unlike bulk Nafion (>20 μm), thin Nafion films can exhibit anomalous physical behavior due to confinement (e.g., interactions between polymer chains and substrate, free surface effects).[14,16,18,21] Along with the anomalous physical processes that occur in thin films, Nafion itself exhibits a convoluted water sorption process, whereby sorption is thought to be governed by a combination of interfacial mass transport limitations, internal diffusion, and polymer swelling dynamics.[22,23] Experimental methods to measure the effect of these factors on water transport in bulk Nafion have involved both steady-state[23,24] and non-steady-state, transient measurements.[23,25] However, there are limited studies probing the effect of these phenomena on water sorption and diffusion in Nafion thin films, where investigations have been limited to transient swelling or water uptake measurements.[5,13,15,16,26] In fact, to date, there are no reported molecular-level measurement techniques that are capable of steady-state diffusion measurements on thin films.

In this study, water vapor diffusion in a Nafion thin film was investigated using time-resolved in situ polarization modulation infrared reflection absorption spectroscopy (PM-IRRAS). Specifically, the diffusion coefficients of both hydrogenated (H_2O) and deuterated (D_2O) water were measured, where switching between the two penetrants was used to deconvolute the effect of polymer dynamics (swelling) on water transport, as well as measure the steady-state, effective diffusion coefficient of water in a nanoscale Nafion film. Unlike other experimental methods used to measure diffusion in thin polymer films (e.g., quartz crystal microbalance (QCM)), PM-IRRAS provides a direct, molecular-level measurement of both Nafion and water in real-time. The physics of the polarization modulation technique (i.e., p-polarized and s-polarized light)[27−29] enables the measurement of water sorption kinetics in humid environments, where only water that is sorbed or diffused

Received: August 20, 2014
Accepted: September 18, 2014
Published: September 24, 2014

   dx.doi.org/10.1021/mz500515b | ACS Macro Lett. 2014, 3, 1029−1035

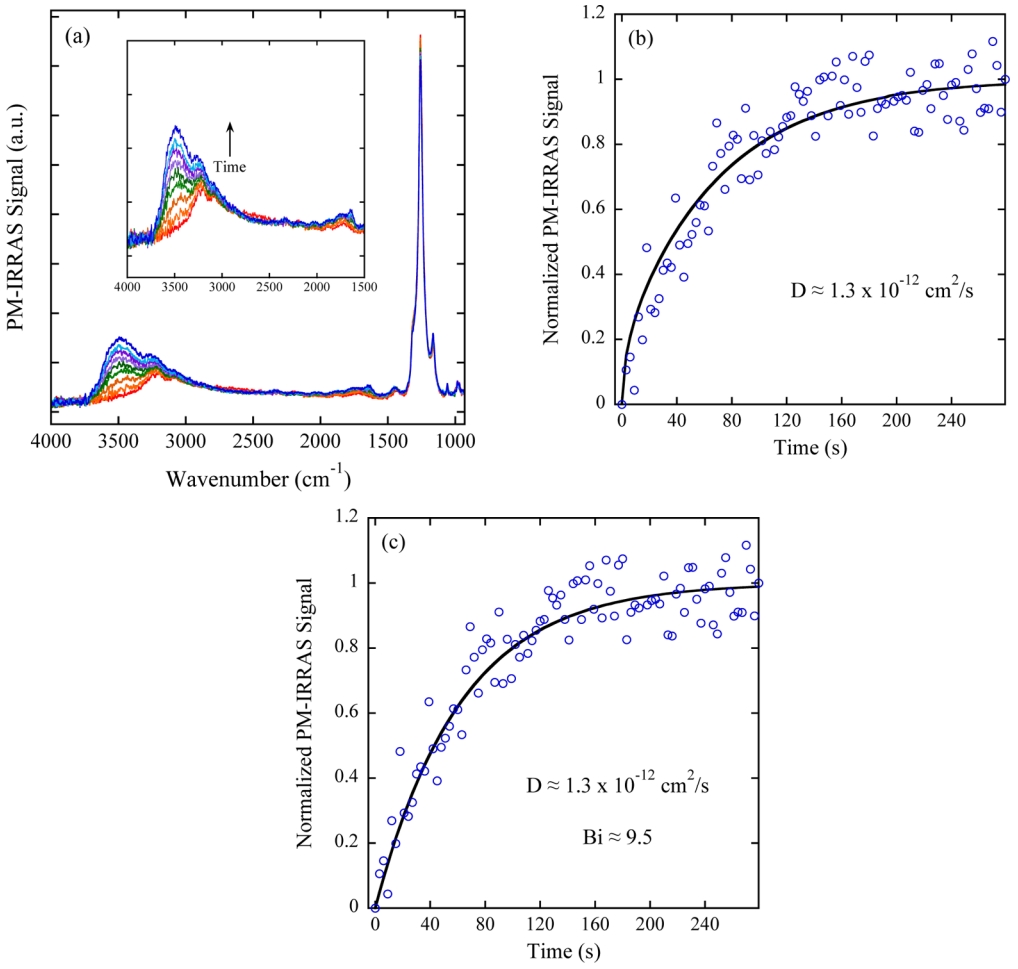

Figure 1. (a) Infrared spectra of H_2O vapor diffusion into a dry Nafion thin film (153 nm) at 25 °C at selected time intervals in response to a relative humidity step of 0% RH to 73% RH. The inset shows the increase of the O−H stretching band (water) with time. Normalized, integrated PM-IRRAS signal of the O−H stretching of water as a function of time at 25 °C, where (b) the solid line represents a regression to the Fickian model (eq 1), where the diffusion coefficient of water, *D*, was the only adjustable parameter, (c) the solid line represents a regression to the Fickian model (eq 2), where the mass-transfer Biot number, Bi, was the only adjustable parameter.

into the Nafion film contributes to the overall infrared signal. Furthermore, with the ability to capture water diffusion in highly hydrated Nafion thin films, contributions from polymer chain relaxations are almost completely eliminated and only internal water diffusion is measured in these thin films. To the best of our knowledge, this is the first time the steady-state, effective diffusion coefficient of water in a hydrated Nafion thin film has been reported.

Figure 1a shows the time-resolved infrared spectra of water vapor diffusing into an initially dry Nafion (equivalent weight: 1100 g Nafion/mol SO_3H) thin film (153 nm ±2 nm; measured by ellipsometry) in response to a relative humidity step of 0% RH to 73% RH at 25 °C. The inset in Figure 1a highlights the infrared region of interest for this study, where the intensity of the water O−H stretching band (broad band between 3720 cm^{-1} and 3325 cm^{-1}) increases with time, representing the sorption and diffusion of water into the Nafion thin film.

In order to calculate the effective diffusion coefficient of water through the Nafion thin film, the experimental water kinetic data was regressed to a 1-D solution to Fick's second law. Since the data obtained from the PM-IRRAS experiments is representative of the concentration profile over the entire film thickness (i.e., the measured infrared signal is position independent since the IR beam travels through the entire film thickness), the PM-IRRAS water uptake data is analogous to that of mass uptake data and can be regressed to the following equation:[30]

$$\frac{I(t) - I_0}{I_f - I_0} = 1 - \sum_{n=0}^{\infty} \frac{8}{(2n+1)^2} \exp\left[\frac{-D(2n+1)^2\pi^2 t}{4L^2}\right] \quad (1)$$

where $I(t)$, I_0, and I_f are the PM-IRRAS signal at any time, the initial, and the final signal, respectively, L is the thickness of the film, and D is the effective diffusion coefficient of water in Nafion (see Supporting Information for full derivation). It must be noted that the diffusion coefficient, D, is referred to as an effective diffusion coefficient in all transport measurements. This terminology is used because there are a number of assumptions that must be made in order to treat the diffusion coefficient as a constant (e.g., film thickness is constant, concentration-independent diffusivity). While this is not the most rigorous treatment of water diffusion in Nafion, this simplified diffusion model sufficiently captures the water uptake kinetics in thin film Nafion (as seen in Figure 1b), without the need for more complicated transport models. Figure 1b shows the normalized (to the final value), integrated PM-IRRAS signal

dx.doi.org/10.1021/mz500515b | ACS Macro Lett. 2014, 3, 1029−1035

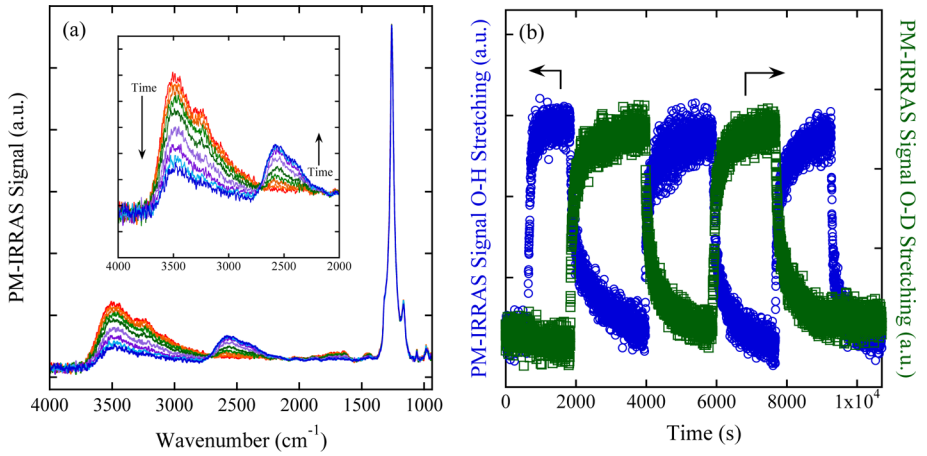

Figure 2. (a) Infrared spectra of a switch between H_2O and D_2O vapor in a hydrated (with H_2O) Nafion thin film at 25 °C at selected time intervals. The inset shows the increase of the O−D stretching band and decrease of the O−H stretching band with time. (b) PM-IRRAS signal of the cycling of H_2O (open blue circles) and D_2O (open green squares) in a Nafion thin film as a function of time.

of the water O−H stretching band as a function of time. The solid black line represents a regression of the water diffusion data to eq 1, where the effective diffusion coefficient, D, was the only adjustable parameter. A value of approximately 1.3×10^{-12} cm^2/s was determined from this regression. While this diffusion coefficient represents the smallest error between experimental data and model (i.e., smallest sum of squared error), the scatter in the water kinetic data (see Figure 1b) allows for a range of effective diffusion coefficients that could adequately fit the data. For Figure 1b, effective diffusion coefficients of 1.3×10^{-12} ($\pm 4 \times 10^{-13}$) cm^2/s provide adequate fits for the water uptake kinetic curve. Similar to previous work on water diffusion in Nafion thin films,[5,15] the diffusion coefficient of water in a 153 nm Nafion film is 4 to 6 orders of magnitude lower than those reported for bulk Nafion (10^{-6} cm^2/s–10^{-8} cm^2/s).[31−34]

Some investigators have reported a mass-transfer resistance (i.e., Biot number $\ll 1$) at the vapor/polymer interface for water diffusion in Nafion.[23,33,35,36] To this end, a first approximation (qualitative analysis) of the experimental setup can be performed. With a water vapor flow rate of over 4 L/min and a sample chamber of about 0.25 L, the exchange rate of vapor inside the sample chamber is sufficiently high (i.e., large convective stream of humidified air), indicating that mass-transfer in the system should be minimal. Furthermore, the mass-transfer Biot number can be directly calculated from a regression of the experimental water uptake data to a solution to Fick's second law, where mass-transfer resistance at the vapor/polymer interface is considered. The resulting equation is as follows:[30]

$$\frac{I(t) - I_0}{I_\infty - I_0} = 1 - \sum_{n=1}^{\infty} \frac{2\mathrm{Bi}^2 \exp(-\beta_n^2 Dt/L^2)}{\beta_n^2(\beta_n^2 + \mathrm{Bi}^2 + \mathrm{Bi})} \quad (2)$$

where Bi is the mass-transfer Biot number and β_n are the positive roots of $\beta \times \tan(\beta) = \mathrm{Bi}$. Figure 1c shows a regression of the water diffusion data to eq 2, where the Biot number, Bi, was the only adjustable parameter (the diffusion coefficient was fixed using the previously calculated value from Figure 1b). A value of 9.5 was determined from this regression, showing that the rate of mass transfer at the vapor/polymer interface is high compared to internal diffusion (see Supporting Information for full Biot number analysis).

While water transport in bulk Nafion films has been extensively studied, there is still much debate on the primary factors that control the rate of water transport in these membranes. Many investigators assume that the rate-limiting factor is internal diffusion of water,[37,38] while others have shown that, depending on membrane thickness and the phases of water to which the membrane is exposed, water transport can be governed by interfacial mass transport limitations, internal diffusion, and polymer swelling (i.e., polymer chain relaxation).[22,23,35] As shown previously, interfacial mass transport resistance (i.e., mass-transfer resistance at the vapor/polymer interface) is not the rate-limiting factor in these experiments, although polymer relaxation (Nafion chain dynamics) can play a significant role in the mechanism of diffusion in these thin films. In order to eliminate polymer chain relaxation, in addition to directly measuring internal water diffusion, a series of switches between H_2O and D_2O were performed. Figure 2a shows the time-resolved spectra of D_2O diffusion in a hydrated (with H_2O) Nafion thin film in response to a relative humidity jump in D_2O of 0% RH to 65% RH at 25 °C.

The inset in Figure 2a highlights the infrared region of interest for this study, where the intensity of the water O−H stretching band (broad band between 3720 cm^{-1} and 3325 cm^{-1}) and water O−D stretching band (broad band between 2750 cm^{-1} and 2100 cm^{-1}) decrease and increase with time, respectively. The increase in intensity of the O−D stretching peak represents the diffusion of D_2O into the Nafion thin film, while the decrease in intensity of the O−H stretching peak represents the diffusion of H_2O out of the Nafion thin film. This data highlights the ability of PM-IRRAS to capture multicomponent transport in a thin polymer film within a single experiment. Figure 2b shows the raw, integrated PM-IRRAS signal of the infrared bands associated with the water O−H stretching (open blue circles) and the deuterium oxide O−D stretching (open green squares) as a function of time. Similar to the spectra presented in Figure 2a, the data shown in Figure 2b represent sorption (increase in PM-IRRAS signal) and desorption (decrease in PM-IRRAS signal) of both H_2O and D_2O during the water transport experiments.

In order to calculate the effective diffusion coefficient of H_2O and D_2O through the Nafion thin film, the experimental water kinetic data was regressed to a 1-D solution to Fick's second

dx.doi.org/10.1021/mz500515b | ACS Macro Lett. 2014, 3, 1029−1035

law (eq 1). A summary of the calculated water diffusion coefficients for both H_2O and D_2O is shown in Figure 3.

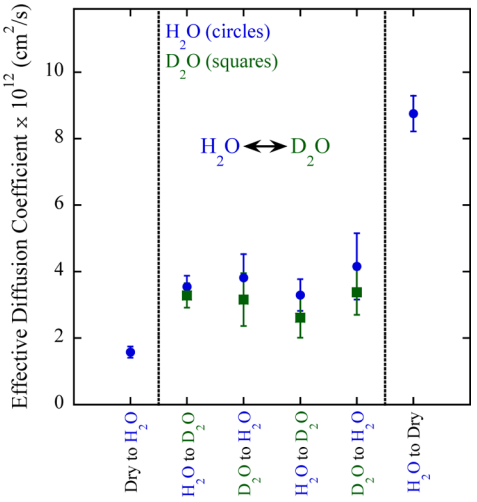

Figure 3. Effective diffusion coefficient of water in the Nafion thin film over a series of switches of H_2O and D_2O at 25 °C. The error bars represent the standard deviation of at least three repeat experiments (in most cases, six repeat experiments).

It should be noted that a value of approximately 176 nm (not 153 ± 2 nm) was used as the hydrated Nafion thickness in all of the calculations of the effective water diffusion coefficients. It was assumed that the Nafion thin film exhibited a swelling ratio of 15%, going from a dry to hydrated state. This is a conservative estimate and represents the lower boundary for water diffusivity since previous researchers have reported swelling ratios of thin film Nafion as high as 20% and 40%.[5,15,39] It was also assumed that negligible swelling and change in water content (ca. 10% change from H_2O to D_2O) of the Nafion thin film occurred during the switch between H_2O and D_2O. This was confirmed by quartz crystal microbalance (see Supporting Information).

It is clear from Figure 3 that three distinct regimes for water diffusion in Nafion are present. The first of these regimes is that of water diffusion into an initially dry Nafion film. Diffusion of water into an initially dry Nafion film would be accompanied by structural rearrangement and swelling (polymer relaxation). This would imply that the calculated water diffusion coefficient for this type of experiment would encompass not only internal diffusion, but also polymer relaxation and rearrangement caused by the diffusion of water into the thin film. It is widely accepted that complete percolation of the ionic domains into connected ionic channels allows for more facile water transport in Nafion, which occurs at elevated humidities.[40,41] Inherently, diffusion into an initially dry Nafion film is slowed down due to the absence of this interconnected ionic network. As a result, the calculated water diffusion coefficient in this first regime is lower than those calculated for the hydrated Nafion film.

The second observed regime represents a series of switches between H_2O and D_2O, where the diffusion coefficient for each diffusing species was calculated within a single transport experiment. It was observed that diffusion within this "hydrated" regime is higher (2−3×) than that in the initially dry Nafion thin film. Again, this difference can be explained by the nanostructure of the Nafion film, where the fully connected network of ionic domains of the initially hydrated film allows for more facile water transport than the unpercolated ionic network of the initially dry thin film. The diffusion coefficient calculated in this second regime represents the steady-state, effective diffusion coefficient of water in a hydrated Nafion thin film. Additionally, it can be seen that the diffusion coefficients for H_2O and D_2O are similar (within experimental error) and can be considered equivalent (small difference may be caused by larger size of the D_2O molecule).

Finally, a third regime is observed, whereby the Nafion film goes from a highly hydrated to fully dry state. The calculated water diffusion coefficient in this regime is over 4 times higher than that of the diffusion coefficient of water in the dry Nafion thin film and more than twice as fast as those calculated for H_2O/D_2O switching experiments. It is believed that the water diffusion coefficient determined for this regime represents only internal diffusion and is not convoluted with such factors as polymer relaxation/rearrangement, which is clearly a factor when going from a dry to hydrated state. To our knowledge, this is the first report where a systematic study was carried out on the factors affecting water transport in an ultrathin (<200 nm) Nafion film (e.g., interfacial mass transport limitations, polymer relaxation), where the diffusion coefficient calculated is representative of pure internal diffusion of water inside the Nafion thin film. This is a critical value for the Nafion community and can be used to help accurately model water diffusion in the catalyst layer of the PEM fuel cell, where again, Nafion is oftentimes confined to nanoscale thicknesses.

Finally, repeat switching experiments were performed on the same Nafion thin film in order to gain further insight into the Nafion thin film chain dynamics (i.e., swelling) during the water sorption process. The use of infrared techniques to measure dilation (relaxation) of a polymer matrix during the diffusion process has been previously established in the literature.[42−44] Figure 4a shows the initially dry and hydrated (with both H_2O and D_2O) spectra of the infrared band associated with the Nafion C−F_2 stretching at 25 °C. These spectra were collected in response to a relative humidity step in H_2O and D_2O of 0%−75% RH and 0%−65% RH, respectively.

Specifically, the Nafion C−F_2 stretching infrared band (located at 1259 cm^{-1}) decreases with time as water (and D_2O) diffuses into the polymer, similar to results observed from previous work on bulk Nafion.[45] From this previous study, the decrease in the C−F_2 stretching band was attributed to water-induced swelling of the Nafion. Physically, as water sorbs into the Nafion thin film, the Nafion swells, increasing the total volume of the sample. The swelling process causes the population of C−F_2 in the sampling region (i.e., the IR beam) to decrease with time, which expresses itself as a decrease in IR intensity of the C−F_2 band. Figure 4b shows the "normalized", integrated PM-IRRAS signal ($I_0/I(t) - 1$) of the infrared band associated with the Nafion C−F_2 stretching (open purple squares) as a function of time. Recent work by Kusoglu and co-workers[26] calculated the swelling (relaxation) time constant to be approximately 30 s for a thin film Nafion (ca. 190 nm) on a gold substrate. To confirm that the decrease in this infrared band with time is due to the swelling of the Nafion thin film, the swelling time constant was calculated for the data in Figure 4b. From this analysis, a swelling (or relaxation) time constant of about 35 s was calculated (shown by the dashed red line). This value is equivalent to that previous calculated for the same material on the same substrate,[26] validating that the decrease in PM-IRRAS signal is purely due to swelling of the Nafion thin film.

dx.doi.org/10.1021/mz500515b | ACS Macro Lett. 2014, 3, 1029−1035

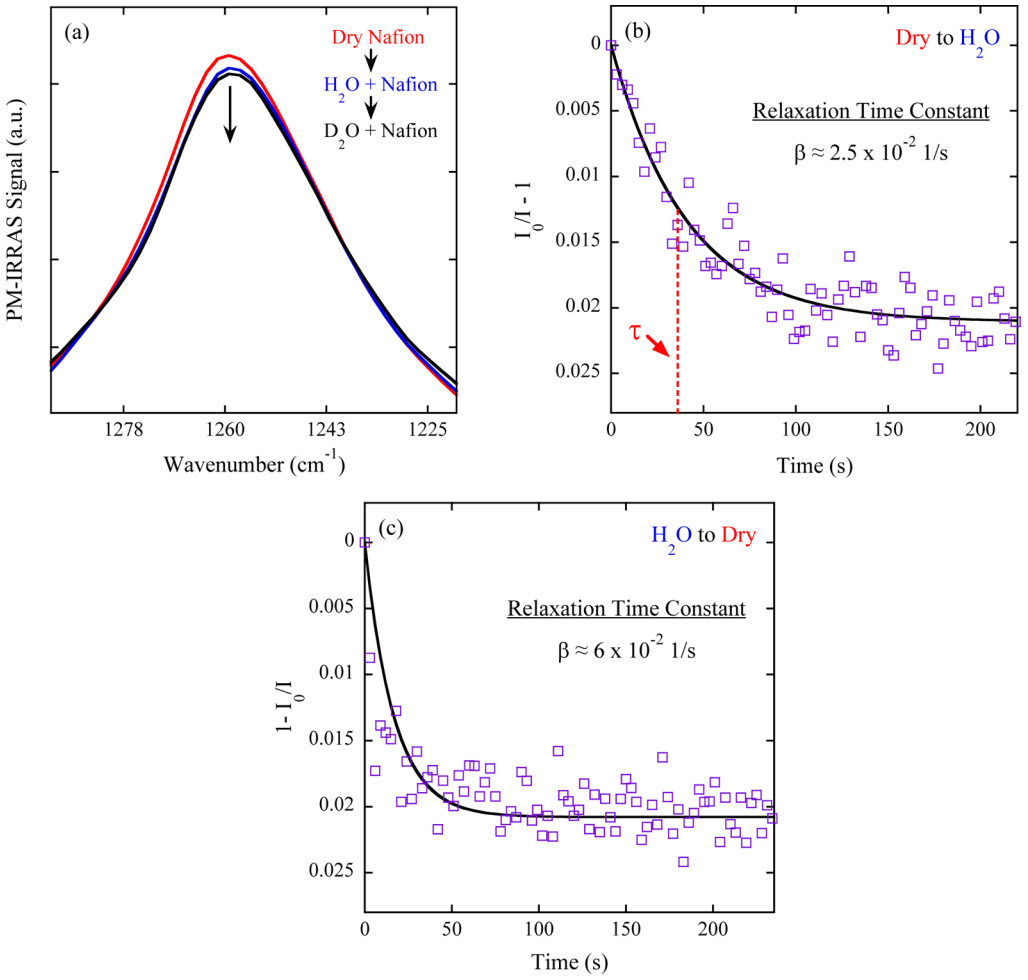

Figure 4. (a) Infrared spectra of the Nafion $C-F_2$ stretching band of dry Nafion (red line), Nafion hydrated with H_2O (blue line), and Nafion hydrated with D_2O (black line) at 25 °C. (b) Regression of the time-resolved Nafion $C-F_2$ stretching absorbance data (purple squares), during initial hydration and (c) during final drying to a polymer relaxation model (eq 3) at 25 °C. The solid line represents the full solution of eq 3, where the relaxation time constant, β, was the only adjustable parameter.

As mentioned above, previous FTIR-ATR studies on water sorption in bulk Nafion (i.e., Nafion 117)[45] showed similar water-induced polymer relaxation (swelling) for both the Nafion backbone ($C-F_2$ bonds) and the Nafion side-chain ($S-O_3$- and $C-O-C$ stretching) during water transport experiments. While swelling of the Nafion side-chains was observed in this study, the signal-to-noise ratio of these IR bands was less than desirable and therefore omitted from the analysis. In the study by Hallinan et al.,[45] the $C-F_2$ polymer data was regressed to a three-element relaxation model in order to calculate a relaxation time constant for this swelling process (i.e., stress dissipated via relaxation of the Nafion matrix). Unlike this previous study, only the early time water uptake data (i.e., less than 300 s) was used in the model regression since only Fickian uptake kinetics was observed in this portion of the data. With this, the $C-F_2$ swelling data of the Nafion thin film can be regressed to a two-element relaxation model (Kelvin (Voigt) model) shown below:

$$\varepsilon = \frac{I_0}{I(t)} - 1 = \frac{\sigma_0}{E}(1 - \exp(-\beta t)) \tag{3}$$

where ε, σ, E, and β are the strain, stress, Young's modulus, and relaxation time constant, respectively. It has been previously shown that the polymer strain is proportional to the change in polymer concentration (i.e., absorbance) due to relaxation.[45−47] Figure 4b shows a regression of the $C-F_2$ stretching PM-IRRAS data, during the initial H_2O hydration, to the Kelvin (Voigt) model (eq 3), where the relaxation time constant, β, was the only adjustable parameter of the regression. A relaxation time constant of about 2.5×10^{-2} 1/s was determined from the regression. In order to compare this value to those obtained for bulk Nafion films, a normalized relaxation time (i.e., polymer chain "diffusion"; $L^2\ \beta$) for the thin Nafion film was determined, where a value of 5.8×10^{-12} cm^2/s was calculated.

The normalized relaxation time calculated for the Nafion thin film is 5-orders of magnitude lower than that of bulk Nafion films (2.7×10^{-7} cm^2/s for Nafion 117). Since water transport and polymer chain dynamics can be coupled (ignoring free-volume effects),[48] a decrease in the Nafion chain dynamics (i.e., slower polymer chain "diffusion") leads to a decrease in water transport in these thin films. This result further highlights the confinement effect that is observed in these thin films,[5,12,14,21] where interactions with the substrate can cause the Nafion chain dynamics to be much slower than those observed in bulk Nafion films. This analysis can be applied to the final drying step (H_2O to dry) in order to discern any correlation between the Nafion chain dynamics and the observed increase in water

dx.doi.org/10.1021/mz500515b | ACS Macro Lett. 2014, 3, 1029−1035

diffusion coefficient. Figure 4c shows a regression of the $C-F_2$ stretching PM-IRRAS data, during the final drying step, to the Kelvin (Voigt) model (eq 3), where the relaxation time constant, β, was the only adjustable parameter of the regression. A relaxation time constant of about 6.0×10^{-2} 1/s was determined from the regression. This value can also be normalized by film thickness, where a value of approximately 2×10^{-11} cm^2/s was determined. The increase in polymer chain "diffusion" (over 3 times faster than initial hydration step) of the Nafion chains during the final desorption step leads to an increase in water diffusivity (see Figure 3), but again, this value is orders of magnitude lower than those calculated for bulk Nafion. The results of the swelling analysis clearly show that Nafion chain dynamics are drastically slowed down in nanoscale films, where this decrease in chain dynamics ultimately leads to a large decrease in water diffusivity.

In summary, water sorption and diffusion in a 153 nm Nafion thin film was captured using time-resolved in situ polarization modulation infrared reflection absorption spectroscopy (PM-IRRAS). Specifically, PM-IRRAS was used to measure the diffusion of both H_2O and D_2O during a series of water sorption experiments where switching between the two penetrants was carried out. The calculated effective diffusion coefficient of water in Nafion was over 4-orders of magnitude lower than those reported for bulk Nafion membranes and was dependent on the initial hydration state of the Nafion; however, little difference was observed between the calculated effective diffusion coefficient for H_2O and D_2O. Additionally, the water-induced swelling data obtained from the water transport experiments was regressed to a relaxation model, where it was observed that Nafion chain dynamics are slowed down significantly compared to chain dynamics in bulk films. This study highlights the powerful capabilities of PM-IRRAS in capturing water diffusion in thin Nafion films and indicates the need for additional studies on the effect of film thickness and polymer film processing on water transport and Nafion chain dynamics in these nanoscale thin films.

■ ASSOCIATED CONTENT

Supporting Information

Experimental description, Nafion thin film preparation, Fickian model derivation, Biot number estimation, and quartz crystal microbalance water uptake data. This material is available free of charge via the Internet at http://pubs.acs.org.

■ AUTHOR INFORMATION

Corresponding Authors

*E-mail: eric.davis@nist.gov.
*E-mail: kirt.page@nist.gov.

Notes

The authors declare no competing financial interest.

■ ACKNOWLEDGMENTS

The authors thank Estefania Quiñones Meléndez and Dr. Brandon Rowe for their initial work on the H_2O to D_2O switching experiments. The authors would also like to thank Dr. Sebastian Engmann and Dr. Nichole Nadermann for their help with ellipsometry and quartz crystal microbalance (QCM), respectively. The National Research Council (NRC) Research Associateship Program (RAP) supported this work.

■ REFERENCES

(1) Mehta, V.; Cooper, J. S. *J. Power Sources* **2003**, *114*, 32−53.
(2) Rikukawa, M.; Sanui, K. *Prog. Polym. Sci.* **2000**, *25*, 1463−1502.
(3) Gottesfeld, S.; Zawodzinski, T. *Adv. Electrochem. Sci. Eng.* **1997**, *5*, 195−301.
(4) Equipment and instruments or materials are identified in the paper in order to adequately specify the experimental details. Such identification does not imply recommendation by the National Institute of Standards and Technology (NIST), nor does it imply the materials are necessarily the best available for the purpose.
(5) Eastman, S. A.; Kim, S.; Page, K. A.; Rowe, B. W.; Kang, S.; Soles, C. L. *Macromolecules* **2012**, *45*, 7920−7930.
(6) Mashio, T.; Malek, K.; Eikerling, M.; Ohma, A.; Kanesaka, H.; Shinohara, K. *J. Phys. Chem. C* **2000**, *112*, 2452−2462.
(7) More, K. L. *DOE Hydrogen Program Annual Progress Report*, DOE: Washington, DC, Nov. 2005.
(8) Siroma, Z.; Ioroi, T.; Fujiwara, N.; Yasuda, K. *Electrochem. Commun.* **2002**, *4*, 143−145.
(9) Siroma, Z.; Kakitsubo, R.; Fujiwara, N.; Ioroi, T.; Yamazaki, S.-i.; Yasuda, K. *J. Power Sources* **2009**, *189*, 994−998.
(10) Bass, M.; Berman, A.; Singh, A.; Konovalov, O.; Freger, V. *Macromolecules* **2011**, *44*, 2893−2899.
(11) Paul, D. K.; Fraser, A.; Pearce, J.; Karan, K. *ECS Trans.* **2011**, *41*, 1393−1406.
(12) Sel, O.; To Thi Kim, L.; Debiemme-Chouvy, C.; Gabrielli, C.; Laberty-Robert, C.; Perrot, H. *Langmuir* **2013**, *29*, 13655−13660.
(13) Dishari, S. K.; Hickner, M. A. *ACS Macro Lett.* **2012**, *1*, 291−295.
(14) Dishari, S. K.; Hickner, M. A. *Macromolecules* **2013**, *46*, 413−421.
(15) Ogata, Y.; Kawaguchi, D.; Yamada, N. L.; Tanaka, K. *ACS Macro Lett.* **2013**, *2*, 856−859.
(16) Modestino, M. A.; Paul, D. K.; Dishari, S.; Petrina, S. A.; Allen, F. I.; Hickner, M. A.; Karan, K.; Segalman, R. A.; Weber, A. Z. *Macromolecules* **2013**, *46*, 867−873.
(17) Paul, D. K.; Karan, K.; Docoslis, A.; Giorgi, J. B.; Pearce, J. *Macromolecules* **2013**, *46*, 3461−3475.
(18) Paul, D. K.; Karan, K. *J. Phys. Chem. C* **2014**, *118*, 1828−1835.
(19) Damasceno Borges, D.; Franco, A. A.; Malek, K.; Gebel, G.; Mossa, S. *ACS Nano* **2013**, *7*, 6767−6773.
(20) Holdcroft, S. *Chem. Mater.* **2014**, *26*, 381−393.
(21) Page, K. A.; Kusoglu, A.; Stafford, C. M.; Kim, S.; Kline, J. R.; Weber, A. Z. *Nano Lett.* **2014**, *14*, 2299−2304.
(22) Satterfield, M. B.; Benziger, J. B. *J. Phys. Chem. B* **2008**, *112*, 3693−3704.
(23) Zhao, Q.; Majsztrik, P.; Benziger, J. *J. Phys. Chem. B* **2011**, *115*, 2717−2727.
(24) Majsztrik, P.; Bocarsly, A.; Benziger, J. *J. Phys. Chem. B* **2008**, *112*, 16280−16289.
(25) Hallinan, D. T., Jr.; Elabd, Y. A. *J. Phys. Chem. B* **2009**, *113*, 4257−4266.
(26) Kusoglu, A.; Kushner, D.; Paul, D. K.; Karan, K.; Hickner, M. A.; Weber, A. Z. *Adv. Funct. Mater.* **2014**, *24*, 4763−4774.
(27) Buffeteau, T.; Desbat, B.; Turlet, J. M. *Appl. Spectrosc.* **1991**, *45*, 380−389.
(28) Green, M. J.; Barner, B. J.; Corn, R. M. *Rev. Sci. Instrum.* **1991**, *62*, 1426−1430.
(29) Buffeteau, T.; Desbat, B.; Blaudez, D.; Turlet, J. M. *Appl. Spectrosc.* **2000**, *54*, 1646−1650.
(30) Crank, J. *The Mathematics of Diffusion*, 2nd ed.; Clarendon Press: Oxford, 1975; pp 47−48.
(31) Takamatsu, T.; Hashiyama, M. *J. Appl. Polym. Sci.* **1979**, *24*, 2199−2220.
(32) Yeagar, H. L.; Steck, A. J. *J. Electrochem. Soc.* **1981**, *128*, 1880−1884.
(33) Majsztrik, P. W.; Satterfield, M. B.; Bocarsly, A. B.; Benziger, J. B. *J. Membr. Sci.* **2007**, *301*, 93−106.
(34) Hallinan, D. T., Jr.; Elabd, Y. A. *J. Phys. Chem. B* **2007**, *111*, 13221−13230.

(35) Adachi, M.; Navessin, T.; Xie, Z.; Hua, L. F.; Tanaka, S.; Holdcroft, S. *J. Membr. Sci.* **2010**, *364*, 183−193.
(36) Kongkanand, A. *J. Phys. Chem. C* **2011**, *115*, 11318−11325.
(37) Rivin, D.; Kendrick, C. E.; Gibson, P. W.; Schneider, N. S. *Polymer* **2001**, *42*, 623−635.
(38) Krtil, P.; Trojanek, A.; Samec, Z. *J. Phys. Chem. B* **2001**, *105*, 7979−7983.
(39) Murthi, V. S.; Dura, J. A.; Satija, S.; Majkrzak, C. F. *ECS Trans.* **2008**, *16*, 1471−1485.
(40) Mauritz, K. A.; Moore, R. B. *Chem. Rev.* **2004**, *104*, 4535−4585.
(41) Devanathan, R.; Venkatnathan, A.; Rousseau, R.; Dupuis, M.; Frigato, T.; Gu, W.; Helms, V. *J. Phys. Chem. B* **2010**, *114*, 13681−13690.
(42) Sammon, C.; Yarwood, J.; Everall, N. *Polymer* **2000**, *41*, 2521−2534.
(43) Giacinti Baschetti, M.; Piccinini, E.; Barbari, T. A.; Sarti, G. C. *Macromolecules* **2003**, *36*, 9574−9584.
(44) Balik, C. M.; Xu, J. R. *J. Appl. Polym. Sci.* **1994**, *52*, 975−983.
(45) Hallinan, D. T., Jr.; De Angelis, M. G.; Giacinti Baschetti, M.; Sarti, G. C.; Elabd, Y. A. *Macromolecules* **2010**, *43*, 4667−4678.
(46) Davis, E. M.; Benetatos, N. M.; Regnault, W. F.; Winey, K. I.; Elabd, Y. A. *Polymer* **2011**, *52*, 5378−5386.
(47) Davis, E. M.; Theryo, G.; Millmyer, M. A.; Cairncross, R. A.; Elabd, Y. A. *ACS Appl. Mater. Interfaces* **2011**, *3*, 3997−4006.
(48) Page, K. A.; Rowe, B. W.; Masser, K. A.; Faraone, A. *J. Polym. Sci., Part B: Polym. Phys.* **2014**, *52*, 624−632.